ON REAL BOUNDED AND REGULAR $(n-k,k)$–LINE KP SOLITONS SUI SOLITONI KP REALI LIMITATI E REGOLARI A $(n-k,k)$ LINEE

SIMONETTA ABENDA

ABSTRACT. After reviewing some of the recent results by S. Chakravarty and Y. Kodama and by Y. Kodama and L. Williams concerning the characterization of the asymptotic behavior of real regular and bounded multi–line soliton solutions to the KP-II equation, we introduce the finite–gap approach to the inverse spectral problem for this family of solutions.

SUNTO. Dopo aver esposto alcuni risultati recenti di S. Chakravarty and Y. Kodama e di Y. Kodama and L. Williams riguardanti la caratterizzazione del comportamento asintotico della famiglia di soluzioni reali limitate e regolari a solitoni multi–linea dell'equazione KP-II, introduciamo l'approccio di tipo finite–gap al problema spettrale inverso per questa famiglia di soluzioni.

2010 MSC. 35Q53; 37K20, 14H70, 14M15.

KEYWORDS. KP-II equation, real multi–line solitons, totally non–negative Grassmannian, asymptotic behavior of solutions, inverse spectral problem

1. INTRODUCTION

The KP equation[17]

$$\text{KP}-\text{II equation}: \ (-4u_t+6uu_x+u_{xxx})_x+3u_{yy}=0, \tag{1}$$

is the first non–trivial flow of the KP integrable hierarchy [34]. Its regular (complex) finite–gap solutions are classified via divisors on non–singular algebraic curves [20], [21] and solutions associated to singular curves, such as solitons, rational solutions, etc., may be obtained as limits from regular complex finite–gap ones [10].

Bruno Pini Mathematical Analysis Seminar, Vol. 8 (2017) pp. 1–25

Dipartimento di Matematica, Università di Bologna

ISSN 2240-2829.

Real regular bounded $(n-k,k)$-line KP solitons, where $k < n$ are positive integers, are solutions to (1) parametrized by a finite set of phases $\kappa_1 < \cdots < \kappa_n$ and by points in $[A]$ in the totally non–negative part of the Grassmannian, $Gr^{\mathrm{TNN}}(k,n) = GL^+_{\mathbb{R}}(k)\backslash Mat^{\mathrm{TNN}}_{\mathbb{R}}(k,n)$. The asymptotic behaviour of these solutions in the (x,y)–plane for any fixed time t has been characterized in [6], [7], while the tropical limit of such solutions for $t \to \pm\infty$ has been related to the combinatorial classification of $Gr^{\mathrm{TNN}}(k,n)$ and to the cluster algebras of Fomin–Zelevinsky[12] in [19].

Real regular finite–gap KP-II solutions correspond to algebraic–geometric data on M–curves: the genus g non–singular curve possesses an anti–holomorphic involution which fixes the maximum number $g+1$ of ovals, *i.e.* it is an M–curve, and the divisor must satisfy the conditions from [11]. An important question is the following: can all real regular KP multisoliton solutions be obtained by degenerating real regular finite-gap KP solutions? In our research project with P.G. Grinevich [3],[4] we provide a positive answer to the above question for all real bounded regular multiline KP solitons.

Plan of the paper: In section 2 we define the Grassmannian, while in section 3 we introduce the representation of points in the totally non–negative Grassmannian via certain weighted oriented graphs following [31]. In section 4 we define $(n-k,k)$–multiline soliton solutions and recall some relevant connections between the asymptotic behavior of such solutions in the (x,y) plane and the combinatorial classification of the totally non–negative Grassmannian established in [7], [19]. Finally in section 5 we introduce the spectral problem for this class of solutions in the Sato Grassmannian and in finite–gap theory.

2. The real Grassmannian

In this section we informally introduce Schubert cell decomposition and Gelfand–Serganova stratification for real Grassmannians. For more details see for instance [13].

Let $k \leq n$ and let $Mat_{\mathbb{R}}(k,n)$ be the set of real $k \times n$ matrices of maximal rank k. Let $GL_{\mathbb{R}}(k)$ be the group of real invertible $k \times k$ matrices. Then the real (k,n) Grassmannian is $Gr(k,n) = GL_{\mathbb{R}}(k)\backslash Mat_{\mathbb{R}}(k,n)$, that is points in $Gr(k,n)$ are equivalence classes of $k \times n$ matrices w.r.t. linear recombinations of the rows.

Let A be a $k \times n$ matrix representing a point $[A] \in Gr(k,n)$. For any k element subset $I = \{1 \leq j_1 < \cdots j_k \leq n\}$ let $\Delta_{(j_1,\ldots,j_k)}(A) := \det(A_I)$ denote the maximal minor formed by the $j_1,\ldots,j_k$ columns of A. If we left multiply A by an invertible matrix with determinant c, then all minors are multiplied by c. Therefore the minors $\Delta_{(j_1,\ldots,j_k)}(A)$ provide local projective coordinates in $Gr(k,n)$, the so called Plücker coordinates and satisfy the Grassmann–Plücker relations

$$\Delta_{(i_1,\ldots,i_k)} \cdot \Delta_{(j_1,\ldots,j_k)} = \sum_{l=1}^{k} \Delta_{(j_l,i_2\ldots,i_k)} \Delta_{(j_1,\ldots,j_{l-1},i_l,j_{l+1},\cdots,j_k)},$$

where $\Delta_{(i_1,\ldots,i_k)} = -|\Delta_{(i_1,\ldots,i_k)}|$ if there is an odd number of elementary transpositions which puts the indeces $i_1,\ldots,i_k$ in increasing order.

$Gr(k,n)$ is decomposed into a disjoint union of Schubert cells Ω_λ indexed by partitions $\lambda \subset (n-k)^k$ whose Young diagrams fit inside the $k \times (n-k)$ rectangle. To each partition $\lambda = (\lambda_1,\ldots,\lambda_k)$, $n-k \geq \lambda_1 \geq \lambda_2 \ldots \geq \lambda_k \geq 0$, $\lambda_j \in \mathbb{Z}$, there is associated a pivot set $I(\lambda) = \{1 \leq i_1 < \cdots < i_k \leq n\}$ defined by the following relations:

$$i_j = n - k + j - \lambda_j, \quad j \in [k]. \tag{2}$$

In the representation of points in $Gr(k,n)$ as non–degenerate $k \times n$ matrices modulo row operations, each Schubert cell is the union of all Grassmannian points sharing the same set of pivot columns I, that is $[A] \in \Omega_{\lambda(I)}$ if and only if I is the lexicographically minimal k–subset of $[n]$ (base) such that $\Delta_I(A) \neq 0$. Indeed, using Gaussian elimination, any $k \times n$ matrix representing a given point in Ω_λ with pivot set I can be transformed by row operations to the canonical (RREF) echelon form, *i.e.* a matrix A such that $A^i_{i_l} = 1$ for $l \in [k]$ and all the entries to the left of these 1's are zero. We may also represent graphically the Schubert cell Ω_λ with a Young diagram, which is a collection of boxes arranged in k rows, aligned on the left such that the j-th row contains λ_j boxes, $j \in [k]$.

The pivot set $I = I(\lambda)$ is given by the k vertical steps in the path along the SE boundary of the Young diagram proceeding from the NE vertex to the SW vertex of the $k \times (n-k)$ bound box. $\bar{I} = [n] \backslash I$ is the non–pivot set. Then the box B_{ij} corresponds to the pivot element $i \in I$ and the non–pivot element $j \in \bar{I}$ (see Figure 1 for an example).

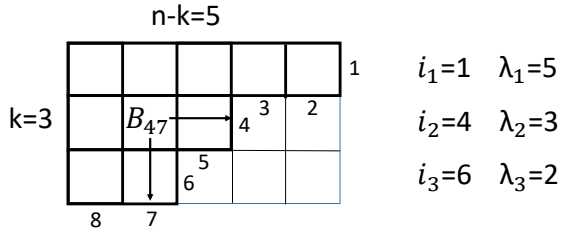

FIGURE 1. *The Young diagram associated to the partition* $(5,3,2)$, $k=3$, $n=8$.

The reduced row echelelon form (RREF) representative matrix for the example in Figure 1 is then

$$A = \begin{pmatrix} 1 & * & * & 0 & * & 0 & * & * \\ 0 & 0 & 0 & 1 & * & 0 & * & * \\ 0 & 0 & 0 & 0 & 0 & 1 & * & * \end{pmatrix}$$

The entries of the RREF matrix provide local affine coordinates for each Schubert cell. Moreover, if we remove all pivot columns and we reflect the result w.r.t the vertical axis we obtain the Young diagram. Therefore the dimension of the Schubert cell Ω_λ is simply the number of boxes of its Young diagram: $\dim(\Omega_\lambda) = \sum_{i=1}^{k} \lambda_i$.

A refinement of this decomposition was proposed in [14], [15]. We recall that a matroid of rank k on the set $[n]$ is a nonempty collection $\mathcal{M}$ of k-element subsets in $[n]$ (bases), that satisfies the exchange axiom: for any $I, J \in \mathcal{M}$ and for any $i \in I$ there exists a $j \in J$ such that $(I \backslash \{i\}) \cup \{j\} \in \mathcal{M}$.

If we index each Plücker coordinate by a base, then each point $[A] \in Gr(k,n)$ is associated to a matroid $\mathcal{M}_{[A]}$ whose bases are the k-subsets I such that $\Delta_I(A) \neq 0$. The exchange axiom is automatically verified thanks to Grassmann–Plücker relations.

Then the refined decomposition of $Gr(k,n)$ into matroid strata[14] is defined by the following rule: each stratum $\mathcal{S}_\mathcal{M} \subset Gr(k,n)$ is composed by the points of the Grassmannian which share the same set of non-zero Plücker coordinates:

$$\mathcal{S}_\mathcal{M} = \{[A] \in Gr(k,n) \,:\, \Delta_I(A) \neq 0 \iff I \in \mathcal{M}\}$$

A matroid $\mathcal{M}$ is called realizable if $\mathcal{S}_\mathcal{M} \neq \emptyset$. The set of the pivot indeces is the lexicographically minimal base of the matroid $\mathcal{M}$.

3. The totally non–negative Grassmannian

In this section we give a brief and incomplete introduction to the totally non–negative Grassmannian following [31], see also [24] for an alternative approach.

Definition 3.1. [31]**The totally non–negative part of** $Gr(k,n)$**.** *The totally non–negative Grassmannian* $Gr^{TNN}(k,n)$ *is the subset of the Grassmannian* $Gr(k,n)$ *with all Plücker coordinates non-negative, i.e. it may be defined as the following quotient:* $Gr^{TNN}(k,n) = GL_k^+ \backslash\ Mat_{kn}^{TNN}$*. Here* GL_k^+ *is the group of* $k \times k$ *matrices with positive determinant, and* Mat_{kn}^{TNN} *is the set of real* $k \times n$ *matrices* A *of rank* k *such that all maximal minors are non-negative, i.e.* $\Delta_I(A) \geq 0$*, for all* k*–element subsets* $I \subset [n] = \{1, \ldots, n\}$*.*

The totally positive Grassmannian $Gr^{TP}(k,n) \subset Gr^{TNN}(k,n)$ *is the subset of* $Gr(k,n)$ *whose elements may be represented by* $k \times n$ *matrices with all strictly positive maximal minors* $\Delta_I(A)$*.*

In [31], Postnikov studies the stratification for $Gr^{\mathrm{TNN}}(k,n)$ analogous to [14].

Definition 3.2. [31]***Positroid cell.*** *The totally nonnegative Grassmann (positroid) cell* $\mathcal{S}_{\mathcal{M}}^{TNN}$ *is the intersection of the matroid stratum* $\mathcal{S}_{\mathcal{M}}$ *with the totally nonnegative Grassmannian* $Gr^{TNN}(k,n)$*:*

$$\mathcal{S}_{\mathcal{M}}^{TNN} = \{\, GL_k^+ \cdot A \in Gr^{TNN}(k,n) \,:\, \Delta_I(A) > 0 \text{ if } I \in \mathcal{M}, \text{ and } \Delta_I(A) = 0 \text{ if } I \notin \mathcal{M} \,\}.$$

The matroid $\mathcal{M}$ *is totally nonnegative if the matroid stratum* $\mathcal{S}_{\mathcal{M}}^{TNN} \neq \emptyset$*.*

Example 3.1. $Gr^{TP}(k,n)$ *is the top dimensional cell and corresponds to the complete matroid* $\mathcal{M} = \binom{[n]}{k}$*.*

In [31] the author introduces many combinatorial objects, like decorated permutations, plabic graphs, necklaces, etc., to represent and characterize positroid cells. In particular, Postnikov introduces the Le–diagrams to represent totally non–negative Grassmann cells.

Definition 3.3. [31]***Le–diagram and Le–tableau.*** *For a partition* λ*, a Le–diagram* D *of shape* λ *is a filling of the boxes of the Young diagram of shape* λ *with* 0*'s and* 1*'s such that, for any three boxes indexed* (i,k)*,* (l,j)*,* (l,k)*, where* $i < l$ *and* $j < k$*, filled*

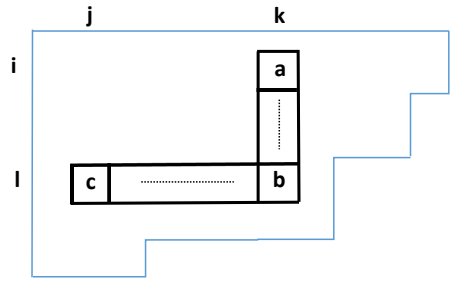

FIGURE 2. *The Le–rule:* $a, c \neq 0$ *imply* $b \neq 0$.

correspondingly with a, b, c*, if* $a, c \neq 0$*, then* $b \neq 0$ *(see Figure 2). For such a diagram denote by* $|D|$ *the number of boxes of* D *filled with* 1*s.*

A Le–diagram is called irreducible *if each column and each row contains at least a 1.*

The Le–tableau T *is obtained from a Le–diagram* D *of shape* λ*, by replacing all 1s in* D *by positive numbers* w_{ij} *(weights).*

An example of Le–tableau is presented in Figure 3. The corresponding Le–diagram is reducible because the column 3 contains only 0s.

Theorem 3.1. [31] *There is a one-to one correspondence between totally non–negative Grassmann cells and Le–diagrams. Moreover, the Le–tableau weights provide a parametrization of any such cell with a minimal number of positive coordinates.*

The explicit relation between totally non–negative Grassmann cells and Le–diagrams may be understood by the representation of the latter by Le–graphs. A Le–graph is a planar directed graph G with a finite number of vertices and edges (see [31] for the definition). A Le–graph (respectively a Le–network) in the disk is associated to any a given Le–diagram (respectively Le–tableau) in the following way. The boundary of the Young diagram of λ gives the lattice path of length n from the upper right corner to the lower left corner of the rectangle $k \times (n-k)$. Place a vertex in the middle of each step in the lattice path and mark the vertices by $b_1, \ldots, b_n$ proceeding NE to SW. The vertices b_i, $i \in I \equiv I(\lambda)$ corresponding to vertical steps are the boundary sources of the network and the remaining vertices b_j, $j \in \bar{I}$, corresponding to horizontal steps are the boundary sinks. Then connect the upper right corner to the lower left corner by another path to obtain a

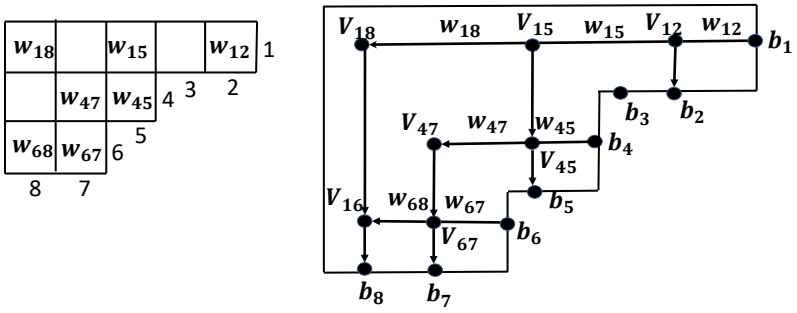

FIGURE 3. *A Le–tableau [left] and its Le–network [right].*

simple close curve containing the Young diagram. For each box of the Le–diagram (i, j) filled by 1, draw an internal vertex V_{ij} in the middle of the box, the vertical line which goes downwards from V_{ij} to the boundary sink and the horizontal line which goes to the right from V_{ij} to the boundary source. By the Le–property any intersection of such lines is also a vertex. All horizontal edges are oriented from right to the left while the vertical edges are oriented downwards. Finally the Le-network from a Le–tableaux of shape λ is simply obtained assigning the weight $w_{ij} > 0$ from the box B_{ij} to the horizontal edge e which enters V_{ij}, and unit weights $w_e = 1$ to all vertical edges. The correspondence between the Le–tableau and the Le-network is illustrated in Figure 3.

The map $T \mapsto N_T$ gives an isomorphism between the set of Le–tableaux T with fixed Le-diagram D and the set of Le-networks (modulo gauge transformations) with fixed graph G corresponding to the diagram D as above.

Definition 3.4. [31]***Boundary measurement map.*** *For each Le–diagram D fitted in a $k \times (n-k)$ rectangle, define the boundary measurement map $Meas_D : T \mapsto Gr^{TNN}(k, n)$ as follows: $\Delta_J(Meas_D(T)) = \sum_{A \in \mathcal{A}_J(N_T)} w(A)$, where*

(1) *J is any k-element subset of $[n]$;*
(2) *N_T is the Le–network corresponding to the Le–tableau T and the boundary source set is labeled by I;*
(3) *$\mathcal{P}_J(N_T)$ is the collection of non–intersecting directed path families $P = \{P_i\}_{i \in I}$ in N_T from the boundary sources I to the boundary destinations J. For any $i \in I \cap J$ the only path to the destination i is path without edges from i to itself, equipped with the weight 1.*

(4) $w(P) = \prod_{i \in I} w(P_i)$;

(5) *the weight of a path* P_i *in the family* P *is the product of the weights* w_e *of the edges* $e \in P_i$: $w(A_i) = \prod_{e \in A_i} w_e$.

Theorem 3.2. *(Theorem 6.5* [31]*) For each Le–diagram as in Definition 3.4 the map* $Meas_D$ *is a well-defined map to the Grassmannian, i.e. the collection* $\Delta_J(Meas_D(T))$ *satisfy Plücker relations, moreover it is a subtraction–free parametrization of a certain totally nonnegative Grassmann cell* $\mathcal{S}_{\mathcal{M}}^{TNN} = Meas_D(\mathbb{R}_{>0}^{|D|}) \subset Gr^{TNN}(k,n)$. *The Le–diagram has shape* λ *if and only if* $\mathcal{S}_{\mathcal{M}}^{TNN} \subset \Omega_\lambda$. *The dimension of* $\mathcal{S}_{\mathcal{M}}^{TNN}$ *is* $|D|$. *Finally, for* D *of shape* λ *the map* $Meas_D$ *is* I*–polynomial, with* $I = I(\lambda)$.

Given a Le–tableau T with pivot set I it is possible to reconstruct both the matroid and the representing matrix in RREF using the Lindström lemma.

Proposition 3.1. [31] *Let* N_t *be the Le–network representing the Le–diagram* D *and let* I *be the pivot set. For any* k*–elements subset* $J \subset [n]$, *let* $K = I \backslash J$ *and* $L = J \backslash I$. *Then the maximal minor* $\Delta_J(A)$ *of the RREF matrix* $A = A(N)$ *is given by the following subtraction–free polynomial expression in the edge weights* w_e*:*

$$\Delta_J(A) = \sum_{Q} \prod_{i=1}^{r} w(Q_i),$$

where the sum is over all non–crossing collections $Q = (Q_1, \dots, Q_r)$ *of paths joining the boundary vertices* b_i, $i \in K$ *with boundary vertices* b_j, $j \in L$.

Let $i_r \in I$, *where* $r \in [k]$ *and* $j \in [n]$. *Then the element* A_j^r *of the matrix* A *is*

$$A_j^r = \begin{cases} 0 & j < i_r, \\ 1 & j = i_r, \\ (-1)^{\sigma_{i_r j}} \sum\limits_{P : i_r \mapsto j} \left(\prod\limits_{e \in P} w_e \right) & j > i_r, \end{cases} \tag{3}$$

where the sum is over all paths P *from the boundary source* b_{i_r} *to the boundary sink* b_j, $j \in \bar{I}$, *and* $\sigma_{i_r j}$ *is the number of pivot elements* $i_s \in I$ *such that* $i_r < i_s < j$.

Finally, it is possible to select $|D|$ positive minors and express all minors of A as a subtraction free rational expression of such basic minors (see also [33] for the explicit construction of one such basis).

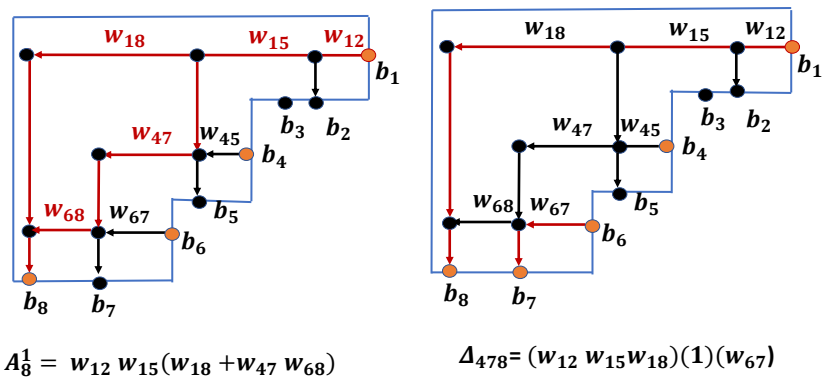

FIGURE 4. *The computation of the matrix entry A^1_8 of the RREF [left] and of the minor $\Delta_{(4,7,8)}(A)$ [right].*

Example 3.2. *Let us consider the Le–diagram D and Le–network as in Figure 3: the pivot set is $I = \{1, 4, 6\}$. The Le–network has 7 non zero entries, it satisfies the Le–property and represents a totally non–negative cell of dimension 7.*

Let A be the RREF matrix representing such point in $Gr^{TNN}(3, 8)$. In Figure 4[left], we explain the computation of the matrix entry A^1_8: it is computed summing the contribution of all weighted directed red paths from the boundary source b_1 to the boundary edge b_8. The sign of such entry is $+$ because one passes two boundary sources - i.e. two pivot columns in the matrix A - to reach the destination b_8.

The minor $\Delta_{(4,7,8)}(A)$ is computed taking all families of non–intersecting paths from the pivot set $I = \{1, 4, 6\}$ to the destination set $J = \{4, 7, 8\}$ (Figure 4[right]): there exists only one such family of non intersecting paths which is evidenced in red.

Finally, it is easy to check that the matrix in reduced row echelon form is

$$A = \begin{pmatrix} 1 & w_{12} & 0 & 0 & -w_{15} & 0 & w_{12}w_{15}w_{47} & w_{12}w_{15}(w_{18} + w_{47}w_{68}) \\ 0 & 0 & 0 & 1 & w_{45} & 0 & -w_{45}w_{47} & -w_{45}w_{47}w_{68} \\ 0 & 0 & 0 & 0 & 0 & 1 & w_{67} & w_{67}w_{78} \end{pmatrix}.$$

The boundary measurement is invariant under the following gauge transformation of the weights w_e [31]: pick a collection of positive real numbers t_v, for any internal vertex $v \in N$ and assume that $t_b = 1$ for each boundary vertex b. Let N' be the network with

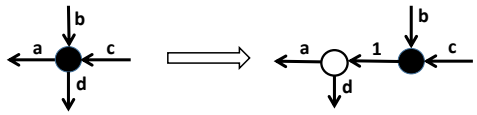

FIGURE 5. *The transformation to a bicolored network at four–valent vertices.*

the same directed graph as N and weights $w'_e = w_e t_u t_v^{-1}$ for each directed edge $e = (u, v)$. Then N' has the same boundary measurement as the network N.

A change of the orientation in N corresponds to a well defined exchange of boundary sources with boundary sinks. If the change of orientation does not effect the orientation of an edge, then that edge keeps the same weight in both orientations, otherwise the weights are reciprocal to each other. Any change of orientation of N corresponds to a change of base in the matroid $\mathcal{M}$ and leaves the boundary measurement map invariant (see [31]).

Any positroid cell is encoded by a decorated permutation [31]. The rule to identify the permutation using the Le–diagram D is explained in [19]: replace each 1 with an elbow and each 0 with a cross; then travel along each pipe from SE to NW and label the end point with the same index as its origin. Finally define the permutation π_D as follows: if i labels a SE horizontal/vertical boundary edge of D then $\pi_D(i)$ labels the NW opposite horizontal/vertical boundary edge of D.

The decorated permutation may be also computed directly from the Le–graph after transforming it to a planar bicolored perfect graph. The rule [31] to transform a four–valent internal vertex into a couple of trivalent black and white vertices is illustrated in Figure 5. The white (respectively black) color is assigned to any internal vertex with one incoming edge (respectively one outgoing edge). Boundary vertices have degree one. Finally one adds internal vertices of degree 2 of convenient color so that each internal edge joins vertices of opposite color.

A planar bicolored network is perfectly orientable if it is possible to assign an orientation to it which respects the coloring rule at the internal vertices. Moreover two planar bicolored perfectly orientable networks in the disk are equivalent if they may be transformed one into the other via a sequence of allowed moves and reductions and equivalent networks share the same boundary measurement [31]. The following criterion allows to

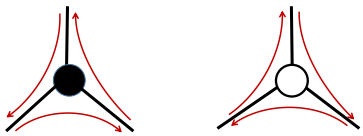

FIGURE 6. *The trip rules at black and white vertices.*

classify equivalent networks: two reduced networks with the same number of boundary vertices may be transformed one into the other using Postnikov moves if and only if they share the same decorated permutation [31]. Such permutation π_N is associated to a given reduced network N independently of its orientation using the trip rule at vertices illustrated in Figure 6.

The following proposition relates the decorated permutations introduced above.

Proposition 3.2. [19] $\pi_D = \pi_N^{-1}$.

We compute π_D and π_N for example 3.2 in Figure 7. In the next section we explain the relation of π_D with the classification of the asymptotic behavior of multi–line KP solitons [19].

4. KP multi–line soliton solutions

In this section we introduce KP multi–line soliton solutions and explain some of their relevant properties following [7] and [19].

Let us fix the following set of data: n phases $\kappa_1 < \cdots < \kappa_n$ and a $k \times n$ real matrix $A \in Mat_{\mathbb{R}}(k,n)$ and let us denote its elements A^i_j with $i \in [k]$, $j \in [n]$. Let

$$f^{(i)}(x,y,t) = \sum_{j=1}^{n} A^i_j E_j(x,y,t), \quad i \in [k], \qquad E_j(x,y,t) = \exp(\kappa_j x + \kappa_j^2 y + \kappa_j^3 t), \tag{4}$$

be a finite set of solutions to the heat hierarchy $\partial_y f = \partial_x^2 f$, $\partial_t f = \partial_x^3 f$. Let us define

$$\begin{aligned} \tau(x,y,t) &= \mathrm{Wr}_x(f^{(1)},\dots,f^{(k)}) \\ &= \sum_{1\le j_1<\cdots<j_k\le n} \Delta_{(j_1,\dots,j_k)}(A) \prod_{1\le r<s\le k} (\kappa_{j_s} - \kappa_{j_r}) \prod_{l=1}^{k} E_{j_l}(x,y,t), \end{aligned} \tag{5}$$

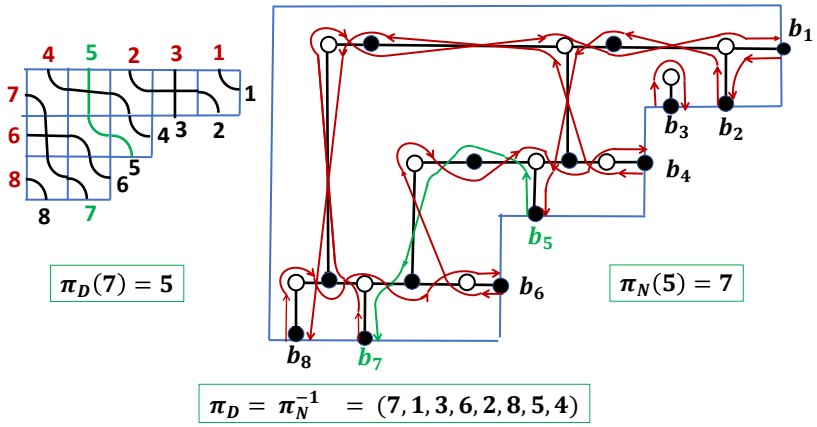

FIGURE 7. *We compute the permutations π_D and π_N for Example 3.2.*

where $\Delta_{(j_1,\dots,j_k)}(A)$ denotes the minor of A formed by the ordered columns $j_1 < \cdots < j_s$. Then

$$u(x, y, t) = 2\partial_x^2 \log(\tau(x, y, t)) \tag{6}$$

is a solution to (1) [26].

Let us remark that we get the same solution if we linearly recombine the rows of A, that is such KP solutions are parametrized by points $[A]$ in the real Grassmannian $Gr(k, n)$.

Comparing (5) and (6), we easily conclude that $u(x, y, t)$ is regular and uniformly bounded for all real (x, y, t) if all Plücker coordinates are non–negative, *i.e.* if $[A]$ is a point of the totally non–negative Grassmannian $Gr^{\mathrm{TNN}}(k, n)$. In [18], the authors prove the untrivial statement that $u(x, y, t)$ is bounded for all real (x, y, t) only if $[A] \in Gr^{\mathrm{TNN}}(k, n)$.

It is not restrictive to suppose that $[A]$ belongs to an irreducible totally non–negative cell. Indeed, using Proposition 3.1, it is easy to check that a zero column in the Le-diagram corresponds to a zero column in the RREF matrix A, *i.e.* the corresponding phase is absent in the solution u, while a zero row in the Le-diagram corresponds to a row in A containing only the pivot term, so that again the corresponding phase plays no role in the solution u.

The simplest example of solution in this class of regular bounded solitons is the one–soliton solution parametrized by the soliton data $\mathcal{K} = \{\kappa_1 < \kappa_2\}$ and $[(1, a)] \in Gr^{\mathrm{TP}}(1, 2)$.

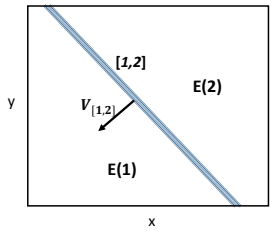

FIGURE 8. *In the (x, y)–plane the one–soliton solution u takes its maximum value $\mathfrak{A}_{[1,2]}$ along the blue line (7) and as time increases the blue line moves in the direction $\vec{V}_{[1,2]}$. In the regions $E(1)$ and $E(2)$ u is approximately zero.*

Let $f(x, y, t) = E_1(x, y, t) + aE_2(x, y, t)$. Then the KP one soliton solution

$$u_{[1,2]}(x, y, t) = \frac{(\kappa_2 - \kappa_1)^2}{2\cosh^2\left(\frac{1}{2}(\kappa_2 - \kappa_1)[x + (\kappa_1 + \kappa_2)y + (\kappa_1^2 + \kappa_1\kappa_2 + \kappa_2^2)t] + \frac{1}{2}\log(a)\right)},$$

for each fixed time $t = t_0$, has its peak along the line

$$x + (\kappa_1 + \kappa_2)y = -\frac{\log(a)}{\kappa_2 - \kappa_1} - (\kappa_1^2 + \kappa_1\kappa_2 + \kappa_2^2)t_0, \tag{7}$$

that is u may be considered a one–line soliton solution. In particular the direction of the line along which the peak occurs does not depend on time t_0. For any fixed time t_0, such line marks the boundary between the region in the (x, y) plane where the exponential E_1 dominates in f from the one where E_2 does. In each such region the KP solution $u(x, y, t_0)$ is approximately zero.

The amplitude $\mathfrak{A}_{[1,2]}$, the wave vector $\vec{\mathfrak{K}}_{[1,2]}$ and the frequency $\mathfrak{O}_{[1,2]}$ respectively are

$$\mathfrak{A}_{[1,2]} = \frac{1}{2}(\kappa_2 - \kappa_1)^2, \qquad \vec{\mathfrak{K}}_{[1,2]} = \left(\frac{1}{2}(\kappa_2 - \kappa_1), \frac{1}{2}(\kappa_2^2 - \kappa_1^2)\right), \qquad \mathfrak{O}_{[1,2]} = \frac{1}{2}(\kappa_2^3 - \kappa_1^3).$$

The soliton velocity vector $\vec{V}_{[1,2]}$ is defined by $\prec \vec{V}_{[1,2]}, \vec{\mathfrak{K}}_{[1,2]} \succ = -\mathfrak{O}_{[1,2]}$, that is

$$\vec{V}_{[1,2]} = -\frac{\kappa_2^2 + \kappa_1\kappa_2 + \kappa_1^2}{1 + (\kappa_2 + \kappa_1)^2}(-1, -(\kappa_1 + \kappa_2)).$$

In particular the x–component of the velocity vector is always negative, that is the line soliton propagates in the negative x–direction. In Figure 8 we show the graph of one such solution.

The first untrivial multi–line soliton solution is the so–called Miles resonance [28]. Let $\mathcal{K} = \{\kappa_1 < \kappa_2 < \kappa_3\}$, $[(1, a_2, a_3)] \in Gr^{\mathrm{TP}}(1, 3)$ and let $f(x, y, t) = E_1(x, y, t) + a_2E_2(x, y, t) + a_3E_3(x, y, t)$. Then, in the plane (x, y), with t fixed, the phases κ_1, κ_2, κ_3,

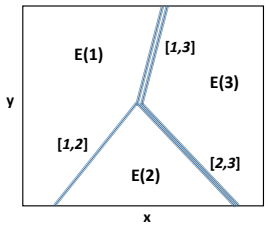

FIGURE 9. *In the (x, y)–plane the (2,1)–soliton solution behaves approximately as a one–soliton solution along each blue semiline.*

respectively dominate for $x \to -\infty$, $-(\kappa_1 + \kappa_2)y < x < -(\kappa_2 + \kappa_3)y$ and $x \to +\infty$ and we label $E[i]$, $i \in [3]$, each such region (see Figure 9). The KP solution $u = 2\partial_x^2 \log(f)$ is approximately zero in each region $E[i]$, $i \in [3]$, and a direct computation shows that, along the semi-line which marks the boundary of the regions $E[i]$ and $[E[j]$,

$$u(x, y, t) \approx u_{[i,j]}(x, y, t),$$

since, along the line $x + (\kappa_i + \kappa_j)y =$ const., the τ–function $f \approx a_i E_i + a_j E_j$.

The three semi–lines meet at a common point (junction vertex) marked by the resonance conditions

$$\vec{\mathfrak{K}}_{[1,3]} = \vec{\mathfrak{K}}_{[1,2]} + \vec{\mathfrak{K}}_{[2,3]}, \qquad \mathfrak{O}_{[1,3]} = \mathfrak{O}_{[1,2]} + \mathfrak{O}_{[2,3]}. \tag{8}$$

In a remarkable series of papers (see [6], [7], [19] and references therein), the authors have succeeded is classifying the asymptotic behavior of soliton data $(\mathcal{K}, [A])$, for generic phases $\mathcal{K} = \{\kappa_1 < \cdots < \kappa_n\}$ and points $[A]$ in the irreducible part of the totally non–negative Grassmannian. Let us summarize the relevant properties of these solutions.

For any fixed time, the plot of the $(n-k, k)$–line soliton solution in the (x, y)–plane, looks like a connected graph with n semilines and finitely many line segments. The complement of such graph consists of finitely many regions each one characterized by a dominant esponential term in the τ function encoded by a base $\{i_1, \ldots, i_k\}$ in the matroid $\mathcal{M}$. Therefore in each such region the solution u is approximately zero. Each line segment or semiline marks the boundary of two adjacent regions and the indeces of the dominant exponentials in the τ–function in adjacent regions are two bases of the form

$\{i, m_2, \ldots, m_k\}$ and $\{j, m_2, \ldots, m_k\}$ [7]. Therefore, along such segment or semiline, the solution is approximately a well–defined one–line soliton solution of type $[i, j]$.

In particular, the asymptotic behavior of the multi–line soliton solutions in the (x, y) plane at fixed time t is combinatorially classified using the permutation π_D introduced in the previous section, under certain technical assumptions on the phases (see [19] for the precise conditions).

Theorem 4.1. [7], [19] *Let $I = \{i_1 < \cdots < i_k\}$ and $\bar{I} = \{j_1 < \cdots < j_{n-k}\}$ respectively be the lexicographically minimal base (pivot set) and its complement in $[n]$ for $[A]$. Let π_D be the permutation of its Le–diagram. Then, the KP solution (6) has the following properties*

(1) *In the unbounded region containing the semiaxis $y = 0$,$x << 0$, the dominant exponential of the τ–function corresponds to the base I;*
(2) *There are k asymptotic line–solitons as $y \to +\infty$, each defined uniquely by the line $[i_l, \pi_D(i_l)]$. From left to right these solitons are listed in decreasing order of the quantity $\kappa_{i_l} + \kappa_{\pi(i_l)}$;*
(3) *There are $(n-k)$ asymptotic line–solitons as $y \to -\infty$, each defined uniquely by the line $[j_s, \pi_D(j_s)]$. From left to right these solitons are listed in increasing order of the quantity $\kappa_{j_s} + \kappa_{\pi(j_s)}$.*

The vertex at which line–solitons meet is generically trivalent and corresponds to a resonant interaction where the balancing condition (8) holds. In [35] there is a vertex dynamics interpretation of this behavior: the solution with one junction vertex may be mapped to its vertex and emulates a free spatially extended particle. Generic solutions show a finite number of junctions each mapped to a vertex. As time t evolves, these vertices move in the (x, y)–plane, collide and then split up. Such collisions may be either elastic or inelastic (see [35] for a partial classification).

The asymptotic behavior in the tropical limit ($t \to \pm\infty$) is thoroughly analyzed in [19]: multi–soliton solutions organize in asymptotic soliton webs formed by line–solitons and soliton junctions which can be described in terms of plane arrangements and cluster algebras naturally associated to the combinatorial classifications of $Gr^{\mathrm{TNN}}(k, n)$. The

reconstruction of soliton data from asymptotic web contour has been analyzed in [9] in the case $Gr^{\mathrm{TP}}(1,n)$ and in [19] in the case $Gr^{\mathrm{TP}}(k,n)$.

5. The spectral approach to real bounded regular multiline KP solitons

Let us recall the construction of the wave function for the KP multi–line soliton solutions. For a general introduction to integrable hierarchies and soliton theory see [8] or [10]. The KP–II equation is part of an integrable hierarchy [34]. In the following we use the following notation $\vec{t}=(t_1,t_2,t_3,t_4,\dots)$ where $t_1=x$, $t_2=y$ and $t_3=t$.

According to Sato theory [32] all KP soliton solutions may be obtained from the dressing (inverse gauge) transformation of the vacuum eigenfunction $\Psi^{(0)}(\zeta,\vec{t})=\exp(\theta(\zeta,\vec{t}))$, which solves

$$\partial_x\Psi^{(0)}(\zeta,\vec{t})=\zeta\Psi^{(0)}(\zeta,\vec{t}),\qquad \partial_{t_l}\Psi^{(0)}(\zeta,\vec{t})=\zeta^l\Psi^{(0)}(\zeta,\vec{t}),\quad l\geq 2,$$

via the dressing (*i.e.* gauge) operator

$$W(\vec{t})=1-\sum_{j=1}^{\infty}\chi_j(\vec{t})\partial_x^{-N},$$

under the condition that W satisfies Sato equations

$$\partial_{t_n}W=B_nW-W\partial_x^n,\qquad n\geq 1,$$

where $B_n=(W\partial_x^nW^{-1})_+$ is the differential part of the operator $W\partial_x^nW^{-1}$. Then

$$L=W\partial_xW^{-1}=\partial_x+\frac{u(\vec{t})}{2}\partial_x^{-1}+\cdots,\qquad u(\vec{t})=2\partial_x\chi_1(\vec{t}),\qquad \hat{\Psi}^{(0)}(\zeta;\vec{t})=W\Psi^{(0)}(\zeta;\vec{t})$$

are respectively the KP-Lax operator, the KP–potential (KP solution) and the KP-eigenfunction, *i.e.*

$$L\hat{\Psi}^{(0)}(\zeta;\vec{t})=\zeta\hat{\Psi}^{(0)}(\zeta;\vec{t}),\qquad \partial_{t_l}\hat{\Psi}^{(0)}(\zeta;\vec{t})=B_l\hat{\Psi}^{(0)}(\zeta;\vec{t}),\quad l\geq 2,$$

where $B_l=(W\partial_x^lW^{-1})_+=(L^l)_+$.

The dressing transformation associated to the line solitons (6) corresponds to the following choice of the dressing operator

$$W=1-w_1(\vec{t})\partial_x^{-1}-\cdots-w_N(\vec{t})\partial_x^{-k},$$

where $w_1(\vec{t}),\dots,w_k(\vec{t})$ are uniquely defined as solutions to the following linear system of equations

$$\partial_x^k f^{(i)} = w_1\partial_x^{k-1} f^{(i)} + \cdots + w_k f^{(i)}, \quad i \in [k]. \tag{9}$$

In such case, $w_1(\vec{t}) = \partial_x\tau/\tau$ and $u(\vec{t}) = 2\partial_x w_1(\vec{t}) = 2\partial_x^2\log(\tau)$. Moreover

$$D^{(k)} \equiv B_k = (L^k)_+ = L^k = \partial_x^k - \partial_x^{k-1}w_1(\vec{t}) - \cdots - w_k(\vec{t}), \tag{10}$$

and $\partial_{t_k} W = 0$.

We observe that $w_1,\dots,w_k$ is the solution to the linear system (9) if and only if

$$D^{(k)} f^{(i)} \equiv W\partial_x^k f^{(i)} = 0, \qquad i \in [k]. \tag{11}$$

Moreover, if the above identity holds, then

$$\partial_{t_l}(D^{(k)} f^{(i)}) = 0, \quad \forall l \in \mathbb{N},$$

that is, by construction, the k-th order Darboux transformation $D^{(k)}$ is associated with the k eigenfunctions $f^{(1)}(\vec{t}),\dots,f^{(k)}(\vec{t})$, of the KP Lax Pair with zero potential for the infinite eigenvalue.

The KP-eigenfunction associated to this class of solutions is

$$\hat{\Psi}^{(0)}(\zeta;\vec{t}) = W\Psi^{(0)}(\zeta;\vec{t}) = \left(1 - w_1(\vec{t})\zeta^{-1} - \cdots - w_k(\vec{t})\zeta^{-N}\right) e^{\theta(\zeta,\vec{t})},$$

or, equivalently,

$$D^{(k)}\Psi^{(0)}(\zeta;\vec{t}) \equiv W\partial_x^k\Psi^{(0)}(\zeta;\vec{t}) = \left(\zeta^k - \zeta^{k-1}w_1(\vec{t}) - \cdots - w_k(\vec{t})\right)\Psi^{(0)}(\zeta;\vec{t}) = \zeta^k\hat{\Psi}^{(0)}(\zeta;\vec{t}). \tag{12}$$

The general method to construct periodic and quasi–periodic solutions to the KP equation is due to Krichever [20, 21]: let Γ be a smooth algebraic curve of genus g with a marked point P_0 and let ζ^{-1} be a local parameter in Γ in a neighborhood of P_0 such that $\zeta^{-1}(P_0) = 0$. The triple $(\Gamma, P_0, \zeta^{-1})$ defines a family of exact solutions to (1) parametrized by degree g non-special divisors $\mathcal{D}$ defined on $\Gamma\backslash\{P_0\}$.

The finite gap solutions of (1) are constructed starting from the commutation representation [34]

$$[-\partial_y + B_2, -\partial_t + B_3] = 0, \tag{13}$$

where

$$B_2 \equiv (L^2)_+ = \partial_x^2 + u, \qquad B_3 = (L^3)_+ = \partial_x^3 + \frac{3}{4}(u\partial_x + \partial_x u) + \tilde{u},$$

and $\partial_x \tilde{u} = \frac{3}{4}\partial_y u$. Then, the Baker-Akhiezer function $\tilde{\Psi}(P, \vec{t})$ meromorphic on $\Gamma\backslash\{P_0\}$, with poles at the points of the divisor $\mathcal{D}$ and essential singularity at P_0 of the form

$$\tilde{\Psi}(\zeta, \vec{t}) = e^{\zeta x + \zeta^2 y + \zeta^3 t + \cdots} \left(1 - \chi_1(\vec{t})\zeta^{-1} - \cdots - \chi_N(\vec{t})\zeta^{-N} - \cdots\right)$$

is an eigenfunction of the following linear differential operators

$$\partial_y \tilde{\Psi} = B_2 \tilde{\Psi}, \qquad \partial_t \tilde{\Psi} = B_3 \tilde{\Psi},$$

and, in such case, imposing compatibility condition (13), $u(\vec{t}) = 2\partial_x \chi_1(\vec{t})$ satisfies the KP equation.

The divisor of poles $\mathcal{D}$ does not depend on the times $\vec{t}$. In contrast to it, the divisor of zeroes $\mathcal{D}(\vec{t})$ depends on all times. The Abel transform of $\mathcal{D}(\vec{t})$ is a linear function of times $\vec{t}$, therefore such transform linearizes the KP hierarchy. $\mathcal{D}$ is an effective divisor, therefore $\Psi(\zeta, \vec{0}) \equiv 1$, and at the point $\vec{t} = \vec{0}$ the divisor of zeroes coincides with the divisor of poles, $\mathcal{D}(\vec{0}) = \mathcal{D}$.

After fixing a canonical basis of cycles $a_1, \ldots, a_g, b_1, \ldots, b_g$ and a basis of normalized holomorphic differentials $\omega_1, \ldots, \omega_g$ on Γ, that is $\oint_{a_j} \omega_k = 2\pi i \delta_{jk}$, $\oint_{b_j} \omega_k = B_{kj}$, $j, k \in [g]$, the KP solution takes the form

$$u(x, y, t) = 2\partial_x^2 \log \theta(xU^{(1)} + yU^{(2)} + tU^{(3)} + z_0) + c_1, \tag{14}$$

where θ is the Riemann theta function and $U^{(k)}$, $k \in [3]$, are vectors of the b–periods of the normalized meromorphic differentials, holomorphic on $\Gamma\backslash\{P_0\}$ and with principal parts $\hat{\omega}^{(k)} = d(\zeta^k) + \ldots$, $k \in [3]$, at P_0 (see [20, 11]).

The necessary and sufficient conditions for the smoothness and realness of the solution (14) associated with smooth curve Γ of genus g have been proven by Dubrovin and Natanzon (see [11] and references therein): Γ must be an M–curve, that is it possesses an antiholomorphic involution

$$\sigma : \Gamma \to \Gamma, \quad \sigma^2 = 1, \quad \sigma(P_0) = P_0, \quad \sigma^*(\zeta) = \bar{\zeta},$$

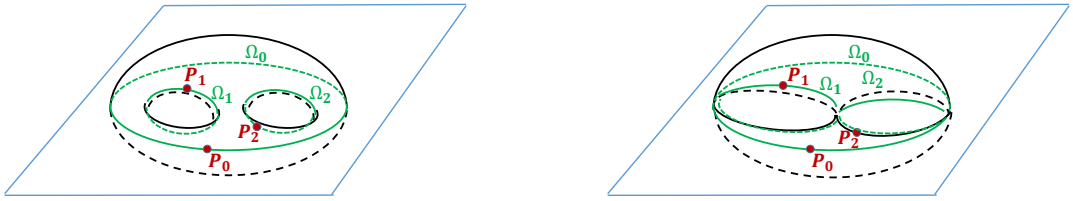

FIGURE 10. *Left: A degree 2 divisor on a regular* M*-curve of genus* $g = 2$ *satisfying the reality and regularity conditions in* [11]. *Right: In the solitonic limit, the spectral curve is a reducible rational* M*–curve and the divisor may still satisfy the reality and regularity conditions.*

where $\bar{\cdot}$ denotes complex conjugation, such that the set of fixed points of σ consists of $g+1$ ovals (the maximum number of ovals [16]), $\Omega_0, \Omega_1, \ldots, \Omega_g$. These ovals are called "fixed" or "real". The set of real ovals divides Γ into two connected components. Each of these components is homeomorphic to a sphere with $g+1$ holes.

On such smooth M–curve of genus g it is possible to fix a basis of cycles such that the essential singularity P_0 belongs to one oval Ω_0 (which is called "infinite" oval), and the remaining g fixed ovals Ω_j, $j \in [g]$ coincide with the a_j-cycles of this basis:

$$\sigma(a_j) = a_j, \quad \sigma(b_j) = -b_j, \qquad j \in [g].$$

We call the ovals Ω_j, $j \in [g]$ "finite". Finally, in order to have regular real quasi–periodic solutions it is necessary and sufficient that each finite oval contains exactly one pole divisor point[11].

For instance, in Figure 10[left] the regular curve has genus 2, the involution is the orthogonal reflection w.r.t. the blue plane and the ovals are green. The reality and regularity conditions from [11] impose that the essential singularity P_0 of the wave–function belongs to one such oval and that there is one simple pole P_i, $i = 1, 2$, in each of the remaining ovals.

Soliton solutions of the KP–II equation correspond to algebraic-geometric data associated to rational curves obtained by shrinking some cycles to double points ([22], see also the book [10] and references therein). In the case of multi–line solitons, it is possible to directly construct such data using the Darboux transformation (10) [25]: the wave

function (12) is defined on a Riemann sphere denoted by Γ_0, and, after normalization, its effective divisor $\mathcal{D}^{(0)} = \{\gamma_l \,; l \in [k]\} \subset \Gamma_0 \backslash \{P_0\}$, consists of real simple poles $\gamma_l \in [\kappa_1, \kappa_n]$ such that

$$(\gamma_l)^k - w_1(\vec{0})(\gamma_l)^{k-1} - \cdots - w_{k-1}(\vec{0})\gamma_l - w_k(\vec{0}) = 0, \qquad l \in [k]. \tag{15}$$

Therefore, the Darboux-Dressing in this finite–dimensional reduction of the Sato Grassmannian provides the following spectral data: a copy of $\mathbb{CP}^1$, Γ_0, with a marked point P_0, n cusps $\kappa_1, \ldots, \kappa_n$, and a real k point divisor $\mathcal{D}^{(0)}$ defined in (15).

Let us now fix $\mathcal{K}$ and let $[A]$ vary in $Gr^{\mathrm{TP}}(k,n)$: we get an $k(n-k)$–dimensional family of real bounded line–solitons. Since such multiline solitons may originate from regular (complex) quasi–periodic finite–gap solutions in the solitonic limit, according to Krichever theorem, we expect that they may be locally parametrized via $k(n-k)$ point divisors on some reducible curve Γ of which Γ_0 is a rational component.

Moreover, the sufficient part of Dubrovin and Natanzon's proof holds also when the algebraic M-curve is singular. Since the multi-soliton solutions associated to points in $Gr^{\mathrm{TNN}}(k,n)$ are real bounded regular for all $\vec{t}$, it is natural to expect that they may be associated to algebraic-geometric data on reducible curves which are rational degenerations of regular M–curves. For example, in Figure 10[right] we show the rational degeneration of the smooth M–curve of Figure 10[left] and the limiting position of the divisor points is in agreement with reality and regularity conditions in [11].

Therefore, in our approach, we consider Γ_0 as a component of some unknown reducible curve Γ and $\mathcal{D}^{(0)}$ as the restriction to Γ_0 of the Krichever divisor of degree $k(n-k)$ on $\Gamma \backslash \{P_0\}$. The main problems we are interested in are the following ones:

(1) Fix generic soliton data $(\mathcal{K}, [A])$ where $\mathcal{K} = \{\kappa_1 < \cdots < \kappa_n\}$ and $[A]$ is a point of a positroid cell $\mathcal{S}^{\mathrm{TNN}}_{\mathcal{M}} \subset Gr^{\mathrm{TNN}}(k,n)$ of dimension $|D|$. Then construct:
   (a) A reducible real algebraic curve Γ which is the rational degeneration of a smooth M–curve of genus $g \geq |D|$ and such that Γ_0 is one of its components,
   (b) Extend the KP wavefunction (12) to a meromorphic function on $\Gamma \backslash \{P_0\}$, in such a way that its effective divisor $\mathcal{D}$ satisfies the reality and regularity

conditions of [11], that is P_0 belongs to one oval and there is exactly one divisor point in each other oval.

(2) Start from Γ, a given rational degeneration of an M–curve, and a Krichever divisor on $\Gamma\backslash\{P_0\}$ satisfying the reality and regularity conditions of [11], then reconstruct the soliton solution, *i.e.* locally parametrize points $[A] \in Gr^{\mathrm{TNN}}(k,n)$ via real and regular divisors on $\Gamma\backslash\{P_0\}$.

Problem (2) is an open untrivial question. Indeed in finite gap theory on smooth irreducible algebraic curves, the effect of moving the divisor points results in a phase shift of the solution $u(x,y,t)$. On the contrary, in the present degenerate setting, moving the divisor points in the ovals may correspond to an untrivial shift from one component to another in the degenerate Jacobian. Any such shift corresponds to a different family of soliton solutions: for instance one may pass from soliton data in $Gr^{\mathrm{TNN}}(k,n)$ to soliton data in $Gr^{\mathrm{TNN}}(k',n')$ with $(k',n') \neq (k,n)$ or even to the trivial KP solution $u(x,y,t) \equiv 0$.

At present, we [2] have been able to characterize an $(n-1)$–parameter family of real regular bounded $(n-k,k)$–line KP solitons in $Gr^{\mathrm{TP}}(k,n)$ parametrized by non–special real divisors on a specific rational degeneration of a genus $g=(n-1)$ hyperelliptic M–curve. These solutions are the so called T–hyperelliptic solitons [5] which are naturally related to the finite Toda lattice [29]. In [1] we have shown that the curve Γ constructed in [3] for soliton data in $Gr^{\mathrm{TP}}(1,n)$ and $Gr^{\mathrm{TP}}(n-1,n)$ is a rational degeneration of a genus $g=(n-1)$ hyperelliptic M–curve. In [2] we use the parametrization by k–compatible divisors of a special $(n-1)$–dimensional variety in $Gr^{\mathrm{TP}}(k,n)$, for any $k \in [n-1]$, and show the relation between the inverse spectral problem of the finite Toda lattice characterized in [23] and the analog problem for T–hyperelliptic solitons.

For what concerns Problem (1), in [3], we have provided an explicit solution in the case $[A] \in Gr^{\mathrm{TP}}(k,n)$ using classical positivity [30]: for any fixed soliton datum $(\mathcal{K},[A])$, we construct a spectral curve Γ, which is the rational degeneration of an M-curve of lowest possible genus $g=k(n-k)$ and a unique KP effective divisor satisfying the reality and regularity conditions.

In [4], we generalize the above result to any soliton datum $[A] \in Gr^{\mathrm{TNN}}(k,n)$ using the representation of $\mathcal{S}^{\mathrm{TNN}}_{\mathcal{M}} \subset Gr^{\mathrm{TNN}}(k,n)$ via networks in the disk proposed in [31]. In

particular, if $[A]$ belongs to a positroid cell of dimension $|D|$, we construct a reducible curve Γ which is the rational degeneration of a smooth $\mathtt{M}$ curve of minimal genus $g = |D|$ and show that the effective divisor of degree $\mathfrak{d} = |D|$ satisfies the reality and regularity conditions following from [11]. In a future publication we plan to compare the asymptotic behavior of the zero divisors points with the multi–line soliton asymptotics established in [7], [9] and [19].

The procedure we use in both papers is constructive: we attach several copies of $\mathbb{CP}^1$ to Γ_0 creating double points and the correct number of ovals, we then extend the vacuum wavefunction $\Psi^{(0)}$ to the curve Γ keeping control of its value at all marked points so to produce a vacuum divisor satisfying appropriate conditions, then, after normalization, the dressed wavefunction satifies the reality and regularity conditions of [11].

Below we briefly illustrate such procedure in the simplest case where $[A] = [a_1 = 1, a_2, a_3] \in Gr^{\mathrm{TP}}(1,3)$. In such case, the curve Γ is the rational degeneration of a hyperelliptic curve of genus 2 (see [3]), with affine part $\{(\zeta,\mu) \,:\, \mu^2 = \prod_{j=1}^3(\zeta-\kappa_j)^2\}$. In figure 11 we show the topological scheme $\Gamma = \Gamma_0 \sqcup \Gamma_1$ of such spectral curve. Let ρ be the hyperelliptic involution and $Q_1 = \rho(P_0)$. For simplicity we use the same symbol to represent the point $p \in \Gamma$ and its ζ coordinate.

Let us extend the vacuum wavefunction to Γ in such a way to create two simple poles in Γ_1

$$\Psi(\zeta;\mathbf{t}) = \begin{cases} \Psi^{(0)}(\zeta;\mathbf{t}) \equiv e^{\theta(\zeta;\mathbf{t})}, & \text{if } \zeta \in \Gamma_0, \\ \Psi^{(1)}(\zeta;\mathbf{t}) \equiv \displaystyle\sum_{j=1}^3 a_j E_j(\mathbf{t})\, \frac{\prod_{s\neq j}(\zeta-\kappa_s)}{(\zeta-b_1)(\zeta-b_2)}, & \text{if } \zeta \in \Gamma_1. \end{cases}$$

The vacuum divisor $\mathbf{B} = \{b_1 < b_2\} \subset \Gamma_1$, is uniquely identified imposing matching conditions at the double points:

$$\Psi^{(0)}(\kappa_j;\mathbf{t}) = \Psi^{(1)}(\kappa_j;\mathbf{t}) = \exp(\theta_j(\mathbf{t})), \quad j \in [3].$$

It is immediate to check that the vacuum divisor of poles satisfies $b_j \in]\kappa_j, \kappa_{j+1}[$, *i.e.* there is exactly one divisor point in each oval. Moreover

$$\Psi^{(1)}(Q_1;\mathbf{t}) \equiv \lim_{\zeta\to+\infty} \Psi^{(1)}(\zeta;\mathbf{t}) = f^{(1)}(\mathbf{t}) = \sum_{j=1}^3 a_j E_j(\mathbf{t}). \tag{16}$$

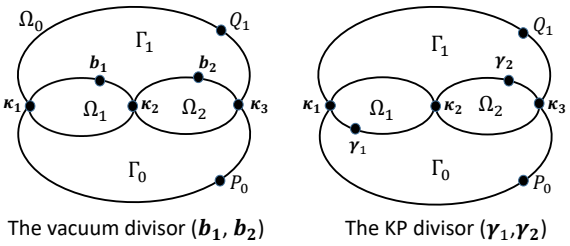

FIGURE 11. *The curve* Γ *and a possible configuration of the vacuum divisor [left] and of the KP divisor [right] for soliton data in* $Gr^{TP}(1,3)$.

In figure 11[left] we show a vacuum divisor satisfying the above properties.

The Darboux transformation $D^{(1)} = \partial_x - \dfrac{\partial_x f^{(1)}(\mathbf{t})}{f^{(1)}(\mathbf{t})}$ applied to the vacuum wavefunction Ψ, acts as a shift on the vacuum divisor of poles and zeroes, *i.e.* it generates a non–effective KP divisor with divisor of poles $\{b_1, b_2, P_0\}$ and divisor of zeros $\{\gamma_1(\vec{t}), \gamma_2(\vec{t}), Q_1\}$, where $\gamma_1(\vec{t}) \in \Gamma_0$ is the Sato zero and $\gamma_2(\vec{t}) \in \Gamma_1$. Indeed

$$D^{(1)}\Psi(\zeta;\mathbf{t}) = \begin{cases} D^{(1)}\Psi^{(0)}(\zeta;\mathbf{t}) \equiv (\zeta - \gamma_1(\vec{t}))e^{\theta(\zeta;\mathbf{t})}, & \text{if } \zeta \in \Gamma_0, \\ D^{(1)}\Psi^{(1)}(\zeta;\mathbf{t}) \equiv \displaystyle\sum_{j=1}^{3} \frac{a_j\kappa_j E_j(\mathbf{t})\prod_{s\neq j}(\zeta-\kappa_s)}{(\zeta-b_1)(\zeta-b_2)} = \\ \qquad = \dfrac{a_1a_2(\kappa_2-\kappa_1)^2E_1(\vec{t})E_2(\vec{t})(\zeta-\kappa_3)+c.p.}{(\zeta-b_1)(\zeta-b_2)}, & \text{if } \zeta \in \Gamma_1. \end{cases}$$

The matching conditions at the double points are satisfied by construction and, moreover, each of the divisor points $\gamma_1(\vec{t})$, $\gamma_2(\vec{t})$ belongs to a distinct finite oval for generic $\vec{t}$ (they may collide at the double point κ_2).

Let $\gamma_i = \gamma_i(\vec{0})$. Then the KP effective divisor $\{\gamma_1, \gamma_2\}$ of the normalized dressed wavefunction

$$\tilde{\Psi}(\zeta;\mathbf{t}) = \frac{D\Psi(\zeta;\mathbf{t})}{D\Psi(\zeta;\mathbf{0})} = \begin{cases} \tilde{\Psi}^{(0)}(\zeta;\mathbf{t}) = \dfrac{\zeta-\gamma_1(\mathbf{t})}{\zeta-\gamma_1}e^{\theta(\zeta;\mathbf{t})}, & \text{if } \zeta \in \Gamma_0, \\ \tilde{\Psi}^{(1)}(\zeta;\mathbf{t}) = \dfrac{A(\vec{t})(\zeta-\gamma_2(\vec{t}))}{\zeta-\gamma_2}, & \text{if } \zeta \in \Gamma_1, \end{cases}$$

satisfies both Sato and Dubrovin–Natanzon constraints.

REFERENCES

[1] S. Abenda. *On KP multi-soliton solutions associated to rational degenerations of real hyperelliptic curves.* Bruno Pini Math. Anal. Semin. 2015, (2015) 138–157.

[2] S. Abenda. *On a family of KP multi–line solitons associated to rational degenerations of real hyperelliptic curves and to the finite non–periodic Toda hierarchy*, J.Geom.Phys. 119 (2017) 112–138.

[3] S. Abenda, P.G. Grinevich. *Rational degenerations of M-curves, totally positive Grassmannians and KP–solitons*, arXiv:1506.00563 submitted.

[4] S. Abenda, P.G. Grinevich. *KP theory, plane–bipartite networks in the disk and rational degenerations of* M*–curves*, arXiv:1801.00208 (2018).

[5] G. Biondini, Y. Kodama. *On a family of solutions of the Kadomtsev-Petviashvili equation which also satisfy the Toda lattice hierarchy.* J. Phys. A **36** (2003) 10519-10536.

[6] S. Chakravarty, Y. Kodama. *Classification of the line-soliton solutions of KPII*, J. Phys. A **41** (2008), no. 27, 275209, 33 pp.

[7] S. Chakravarty, Y. Kodama. *Soliton solutions of the KP equation and application to shallow water waves*, Stud. Appl. Math. **123** (2009) 83-151.

[8] L. A. Dickey. Soliton equations and Hamiltonian systems. Second edition. Advanced Series in Mathematical Physics, **26** World Scientific Publishing Co., Inc., River Edge, NJ, 2003. xii+408 pp.

[9] A. Dimakis, F. Müller-Hoissen. *KP line solitons and Tamari lattices.* J. Phys. A **44** (2011) 025203 49 pp.

[10] B.A. Dubrovin, I. M. Krichever, S.P. Novikov. Integrable systems. in Dynamical systems IV, Encyclopaedia Math. Sci., 4, Springer, Berlin, (2001), 177-332.

[11] B. A. Dubrovin, S. M. Natanzon. *Real theta-function solutions of the Kadomtsev-Petviashvili equation.* Izv. Akad. Nauk SSSR Ser. Mat., **52** (1988) 267-286.

[12] S. Fomin, A. Zelevinsky. *Cluster algebras I: foundations.*, J. Am. Math. Soc. **15** (2002) 497-529.

[13] W. Fulton. Young tableaux. Cambridge University Press (1997).

[14] I. M. Gel'fand, R. M. Goresky, R. D. MacPherson, V. V. Serganova. *Combinatorial geometries, convex polyhedra, and Schubert cells.* Adv. in Math. **63** (1987) 301–316.

[15] I. M. Gel'fand and V.V. Serganova. *Combinatorial geometries and torus strata on homogeneous compact manifolds.*Russian Mathematical Surveys, **42** (1987) 133–168.

[16] B. H. Gross, J. Harris. *Real algebraic curves*, Ann. Sci. École Norm. Sup. série 4, **14** (1981), 157–182.

[17] B.B. Kadomtsev, V.I. Petviashvili. *On the stability of solitary waves in weakly dispersive media.* Sov. Phys. Dokl. **15** (1970) 539-541.

[18] Y. Kodama, L. Williams. *The Deodhar decomposition of the Grassmannian and the regularity of KP solitons*, Adv. Math. **244** (2013) 979-1032

[19] Y. Kodama, L. Williams. *KP solitons and total positivity for the Grassmannian*, Invent. Math. **198** (2014), no. 3, 637-699

[20] I. M. Krichever. *An algebraic-geometric construction of the Zakharov-Shabat equations and their periodic solutions.* (Russian) Dokl. Akad. Nauk SSSR, **227** (1976) 291-294.

[21] I. M. Krichever. *Integration of nonlinear equations by the methods of algebraic geometry.* (Russian) Funkcional. Anal. i Prilozen., **11** (1977) 15-31, 96.

[22] I. M. Krichever. *Spectral theory of nonstationary Schroedinger operators and non stationary Peierls model.* Funk.anal. i pril. **20** (1986) 42–54.

[23] I. M. Krichever, K. L. Vaninsky. *The periodic and open Toda lattice.* AMS/IP Stud. Adv. Math., **33**, Amer. Math. Soc., Providence, RI, (2002) 139–158.

[24] T. Lam. *Totally nonnegative Grassmannian and Grassmann polytopes.* in Current developments in mathematics 2014, Int. Press, Somerville, MA, (2016) 51–152.

[25] T. M. Malanyuk. *A class of exact solutions of the Kadomtsev-Petviashvili equation*, Russian Math. Surveys **46** (1991) 225–227.

[26] V. B. Matveev, M. A. Salle. Darboux transformations and solitons., Springer Series in Nonlinear Dynamics. Springer-Verlag, Berlin, (1991).

[27] E. Medina. *An N Soliton Resonance Solution for the KP Equation: Interaction with Change of Form and Velocity.* Lett. Math. Phys. **62** (2002) 91–99.

[28] J. W. Miles. *Diffraction of solitary waves.* J. Fluid. Mech. **79** (1977) 171–179.

[29] J. Moser. *Finitely many mass points on the line under the influence of an exponential potential - an integrable system.* in Dynamical systems, theory and applications, Lecture Notes in Phys. **38**, Springer, Berlin (1975), 467-497.

[30] A. Pinkus. Totally positive matrices, Cambridge Tracts in Mathematics, vol. 181, Cambridge University Press, Cambridge, (2010).

[31] A. Postnikov. *Total positivity, Grassmannians, and networks.*, arXiv:math/0609764 [math.CO].

[32] M. Sato. Soliton equations as dynamical systems on infinite-dimensional Grassmann manifold, in: Nonlinear PDEs in Applied Sciences (US-Japan Seminar, Tokyo), P. Lax and H. Fujita eds., North-Holland, Amsterdam (1982), 259-271.

[33] K. Talaska. *Combinatorial formulas for* Γ*–coordinates in a totally nonnegative Grassmannian*, J. Combin. Theory Ser. A **118** (2011) 58–66.

[34] V. E. Zakharov, A. B. Shabat. *A scheme for integrating the nonlinear equations of mathematical physics by the method of the inverse scattering problem. I*, Funct. Anal. and Its Appl., **8** (1974) 226-235.

[35] Y. Zarmi. *Vertex dynamics in multi-soliton solutions of Kadomtsev-Petviashvili II equation.* Nonlinearity **27** (2014), 1499-1523.

Dipartimento di Matematica, Università di Bologna

E-mail address: simonetta.abenda@unibo.it